



Designing a modelling structure for the grapevine downy mildew pathosystem

Federica Bove · Serge Savary · Laetitia Willocquet · Vittorio Rossi

Accepted: 6 April 2020 / Published online: 15 May 2020
© Koninklijke Nederlandse Planteziektenkundige Vereniging 2020

Abstract A process-based simulation model for the grapevine-downy mildew pathosystem was developed in order to quantitatively synthesize the literature available and to provide a tool to guide strategic decisions for disease management. The model includes: i) the main processes involved in the disease dual epidemics on leaves and clusters, from inoculum mobilisation to disease multiplication on foliage, and to infection of clusters; and ii) host dynamics, i.e. crop development, growth, and physiological and disease-induced senescence. A numerical evaluation was performed to investigate the response of the model to changes of the main epidemiological parameters, i.e. the basic infection rate corrected for the removals (R_{cOPT}), the duration of latency period (LP), the duration of infectious period (IP), and the rate of primary infections (P). Increasing values of R_{cOPT} and IP, and decreasing values of LP resulted in a faster increase of the epidemic on both foliage and clusters, while decreasing values of P delayed epidemics. The simulated dynamics of epidemics on foliage and clusters conformed to patterns of dual epidemics observed for downy mildew. The model can be useful for investigating the effect of strategic

disease management tools such as the use of resistant varieties or to investigate the behaviour of the pathosystem under scenarios of climate change.

Keywords Modelling framework · *Plasmopara viticola* · Simulation modelling · Systems analysis · *Vitis vinifera*

Introduction

Downy mildew (DM), caused by the Oomycete *Plasmopara viticola* (Berk. & Curt.) Berl. & de Toni, is one of the most important grapevine diseases worldwide (Gessler et al. 2011). *Plasmopara viticola* affects both leaves and clusters, and causes yield and quality losses. DM is a polycyclic disease in which sexual and asexual spores cause primary and secondary infections, respectively (Gobbin et al. 2001, Gobbin et al. 2003).

Many studies have been conducted on the epidemiological processes leading to grapevine DM epidemics, and on the many factors influencing them. These processes operate within a hierarchy (Zadoks and Schein 1979) and concern different levels of integration (Rabbinge and de Wit 1989), such as spore germination and infection (respectively at the levels of the pathogen spore and of the host plant site), lesion development (at the leaf or grape cluster levels), and disease progress (at the whole plant and vineyard levels). These levels of integration differ in their physical scales, and also in their temporal characteristics, from minutes (e.g., spore germination) to months (e.g., an epidemic).

F. Bove · V. Rossi (✉)
DIPROVES, Università Cattolica del Sacro Cuore, Piacenza, Italy
e-mail: Vittorio.rossi@unicatt.it

S. Savary · L. Willocquet
INRA, AGIR, Centre de Toulouse-Occitanie, Université de
Toulouse, INPT, INP- EI Purpan, Castanet-Tolosan, France

Simulation models are developed with the main objectives of synthesizing the current knowledge on processes and interactions involved in a given system, better understanding the system behaviour, and identifying knowledge gaps. Simulation models have further been used to guide tactical or strategic decisions to manage the system of interest (Shoemaker 1981). Models designed to produce a quantitative synthesis of the available knowledge of crop disease epidemics have, for example, been described for hop downy mildew (Royle 1973), apple scab (Kranz 1979), apple powdery mildew (Jeger 1984), groundnut rust (Savary et al. 1990), bean angular leafspot (Allorent et al. 2005; Allorent and Savary 2005), rice sheath blight (Savary et al. 2012), *Septoria tritici* blotch of wheat (Savary et al. 2015), and coffee diseases (Avelino et al. 2018). The model developed by Rossi et al. (2009) for grapevine DM simulates epidemics to understand the role of primary and secondary infections on the epidemic development. This model however does not consider other features of DM epidemics such as, for instance, the dual nature of DM epidemics (Savary et al. 2009) on both leaves and clusters.

In the field of disease management, tactical models aim to provide short-term and field-scale predictions (Zadoks and Rabbinge 1985) of disease dynamics and their impact on harvests in order to guide decisions (e.g., fungicide applications, Kranz and Hau 1980). Some tactical models have been developed for grapevine DM (Gessler et al. 2011), focusing on primary infections (Hill 1990, 2000; Park et al. 1997; Rossi et al. 2005; Rossi et al. 2008) or dealing with the development of secondary infections through the simulation of one or more processes of the biological cycle of *P. viticola* (Blaise et al. 1999; Ellis et al. 1994; Kassemeyer 1994; Lalancette et al. 1988; Magarey et al. 1991; Orlandini et al. 1993). The model developed by Leroy et al. (2013) simulates DM epidemics on both leaves and clusters resulting from both primary and secondary infections, and incorporates yield losses and grower's income, as influenced by weather conditions and fungicide applications. All these tactical models have been designed for application in specific conditions, and require specific environmental input data, and a number of parameters that make them site- and vineyard-specific. Strategic models have a main purpose of identifying the importance of a particular component involved in the system, and to quantify the consequences of disease management actions in general, including long-term decisions,

such as the choice of a (resistant) variety. Such models have not been developed for DM.

The objective of this work is to develop a generic modelling structure for grapevine DM epidemics, which encompasses the main phases of the disease epidemiological processes, from inoculum mobilisation to disease multiplication on the foliage, and to infection of clusters. This structure is meant to capture some of the main features of the disease, and to mobilize available data from the literature. This structure is also meant to be used to analyse the respective contributions of different phases of the disease (i.e., primary infections vs. secondary infections), the linkages between disease processes (e.g., disease on foliage relative to disease on clusters, an element that is missing in most of the previously mentioned models), and the effects of host dynamics (growth and senescence) on disease development.

Materials and methods

This section describes the main specifications of the model, the model blueprint and structure, as well as the approach used for a numerical evaluation of the model. The resulting model is described in the Results section.

Specifications of the model

We developed a model structure using the following specifications: (1) consideration of a few, but critical disease epidemiological processes; (2) inclusion of the main host crop processes, i.e., crop growth and senescence, as well as crop development and fruit (cluster) formation; (3) consideration of a suitable system size, that is to say, large enough to include a series of plant and pathogen associated elements, which encapsulate the key components of a DM epidemic, i.e., foliage, clusters, primary inoculum, lesions, and secondary inoculum; (4) responses to key environmental variables represented by driving functions for both the physical environment and for crop management actions; (5) consideration of a suitable time frame, that is to say, a time duration enabling to address the annual dynamics of a DM epidemic on a growing grapevine; (6) use of a time step that accounts for weather variability and rhythm, so that disease (specification 1) and crop (specification 2) are modelled as continuous processes.

Model blueprint

The DM-grapevine pathosystem involves a large number of interactions occurring at different levels of hierarchy. The design of a system model implies simplifications that are incorporated into the model as assumptions. These assumptions are meant to enable the design of the model, which is envisioned as a simplification of the reality (Forrester 1997; Zadoks 1971). A number of these assumptions–simplifications are described in the following blueprint, according to the model specifications; their rationale is addressed in the discussion section.

Key disease epidemiological processes

The model elaborates on the foundations established by Vanderplank (1963) with the processes of infection, latency, and infectiousness, summarized in:

$$dx_t/dt = R_c (x_{t-p} - x_{t-i-p}) (1 - x_t) \quad (1)$$

where: x_t is the proportion of infected tissue at time t , R_c is the basic infection rate corrected for the removals (i.e. tissue removed from the infectious process), p is the latency period, and i is the infectious period.

The latency period (p) is the delay, in days, within which newly infected tissue becomes infectious. The infectious period (i) is the time interval, in days, during which a lesion produces new spores and is able to generate new infections. A lesion that no longer produces spores is removed from the epidemic process (Zadoks and Schein 1979).

In eq. (1), the term $(x_{t-p} - x_{t-i-p})$ corresponds to the infectious fraction of x_t . This term is multiplied by R_c , which represents the number of daughter lesions per mother lesion per unit time with the dimension $[N_{les} \cdot N_{les}^{-1} \cdot T^{-1}]$. R_c corresponds to the effective dispersal unit per infection unit per unit time. R_c is the product of the relative rate of spore production (N) in number of spores per lesion per day, with dimension $[N \cdot N^{-1} \cdot T^{-1}] = [T^{-1}]$, and of the effectiveness (E) of each pathogen propagule in causing new infection, with dimension $[N \cdot N^{-1}] = [1]$ (Zadoks and Schein 1979); therefore:

$$R_c = N \times E \quad (2)$$

In eq. (1), the infectious fraction of x_t is also multiplied by the “correction factor” $(1 - x_t)$ (Zadoks 1971),

which is the proportion of healthy tissue that is still available for infection. The correction factor is bound between 0 and 1, where 1 corresponds to the carrying capacity of the system.

The concepts established by Vanderplank have been translated into botanical epidemiology by Zadoks (1971). The host crop consists of a number of sites, which may be partitioned in several, non-overlapping categories: (1) healthy sites (HS); (2) sites which have been infected but are not yet infectious, and therefore are latent (L); (3) sites that are infectious and are generating secondary infections (I); and (4) sites that are no longer infectious and thus are removed from the infectious sites (R). The notion of site refers to a portion of plant tissues that can sustain a given infection and potentially give raise to new ones (Vanderplank 1963). In the case of grapevine downy mildew, a site corresponds to a tissue that can sustain a lesion.

The present model addresses disease progress both on leaves and clusters. Inclusion in the model of the infection process on clusters is important to understand the linkage between components of dual epidemics. In the case of DM, a nonlinear relationship links foliage and clusters (Savary et al. 2009). Clusters are considered in two possible states only: healthy or infected.

Main host processes

The model includes crop growth and senescence in the simplest possible way. Crop growth and senescence are major causes for epidemiological variability (Zadoks and Schein 1979), with strong effects of host dynamics on disease development (Campbell and Madden 1990; Vanderplank 1963; Zadoks and Schein 1979).

Crop growth is represented as the progressive increase in healthy sites during the crop cycle, and is reflected by a logistic increase for foliage growth. Senescence is represented as the physiological process that leads to fewer sites being available for infection as the foliage ages. The model considers both physiological and disease-induced senescence on the foliage, the latter being caused by a reduction of photosynthesis and an alteration of the carbon balance of the host crop caused by the disease (Caffi et al. 2010; Farrar 1992; Giuntoli and Orlandini 2000).

Crop development and age are also included into the model, in order to account for changes in host susceptibility, both for leaves and clusters (Kennelly et al. 2005; Reuveni 1998). Crop development is the passing of the

crop through successive, physiologically different stages (Zadoks and Schein 1979). The change in host susceptibility with crop age is known as ontogenic resistance (Develey-Rivière and Galiana 2007; Ficke et al. 2002; Kennelly et al. 2005).

System size

A system is a well-defined segment of reality, separated from the outside environment by clear boundaries (Zadoks 1971). The system under consideration is a single grapevine plant surrounded by similar grapevine plants in term of size, physiology and development, and disease.

The size of the system is defined by LA, the maximum leaf area deployed by the considered reference grapevine plant of the system, and by NC, the number of clusters borne by this plant. LA further enables the calculation of the maximum number of sites present in the system, as: $S_{max} = LA/LS$, where LS is the area of each individual DM lesion, i.e., the size of a [foliage] site. At the beginning of each simulation, the size of the foliage component is set to 100 healthy sites.

Driving functions

Driving functions represent the environmental factors that may influence the functioning of the considered system (weather, soil, but also crop management) (Rabbinge and de Wit 1989; Savary and Willocquet 2014). Environmental factors may be considered, as here, in a scenario approach. We consider weather variables, which are represented in sets of environmental scenarios, by fixed levels of temperature and moisture (which includes both rainfall and leaf wetness duration) throughout a run duration over the time frame of a growing season (i.e., 200 days). Using this approach, each environmental scenario corresponds to sets of associated values for epidemiological parameters involved in both primary (inflow of primary infections, onset date of primary infections, period of primary inoculum mobilization) and secondary infections (latency and infectious periods, modifiers of the corrected basic infection rate for temperature and moisture). In each run, which is performed along a given environmental scenario, these epidemiological parameters are fixed.

In the present work, we considered only one environmental scenario, which is highly conducive to disease. Several runs of the model in different climatic

scenarios that are more or less conducive for the disease development are reported in Bove (2018; Bove et al. Submitted).

Epidemic time frame

Epidemics are simulated over a 200-day period, covering the growing season from bud break until leaf-fall. Bud break (stage 07 of Lorenz et al. 1995) is assumed to occur on April 1st (day of year, DOY 90) with northern Italy as the reference environment (Poni et al. 2006). The simulation ends on October 17th (DOY 289), which approximately corresponds to the end of leaf-fall (stage 97) in northern Italy (Poni et al. 2006).

Time step

The operational definition for a time step is a small fraction of the time frame in which the rates in the considered system are not likely to change strongly (i.e., change by more than 50% of their value; Rabbinge and de Wit 1989; Savary and Willocquet 2014; Zadoks 1971). In this work, epidemics are simulated on a daily time step, which is sufficient to capture the main features of disease processes and plant growth.

Model structure: Main components and their relationships

The general structure of the model consists of five main components: 1) primary infections; 2) lesions on foliage (resulting from both primary and secondary infections); 3) secondary infections; 4) lesions on clusters; and 5) crop growth and development. Relationships between these model components are summarized in Fig. 1. Primary infections increment the number of lesions on leaves; lesions on leaves generate secondary infections on leaves and on clusters. Infections on clusters are assumed to not give rise to new infections neither on leaves or clusters. The number of sites on leaves is dynamic during the season, and is influenced by crop growth and senescence. Leaves may vary in their susceptibility with age, which depends on crop development. Crop development plays also an important role on disease dynamics on clusters, by determining the period during which clusters are susceptible to infection.

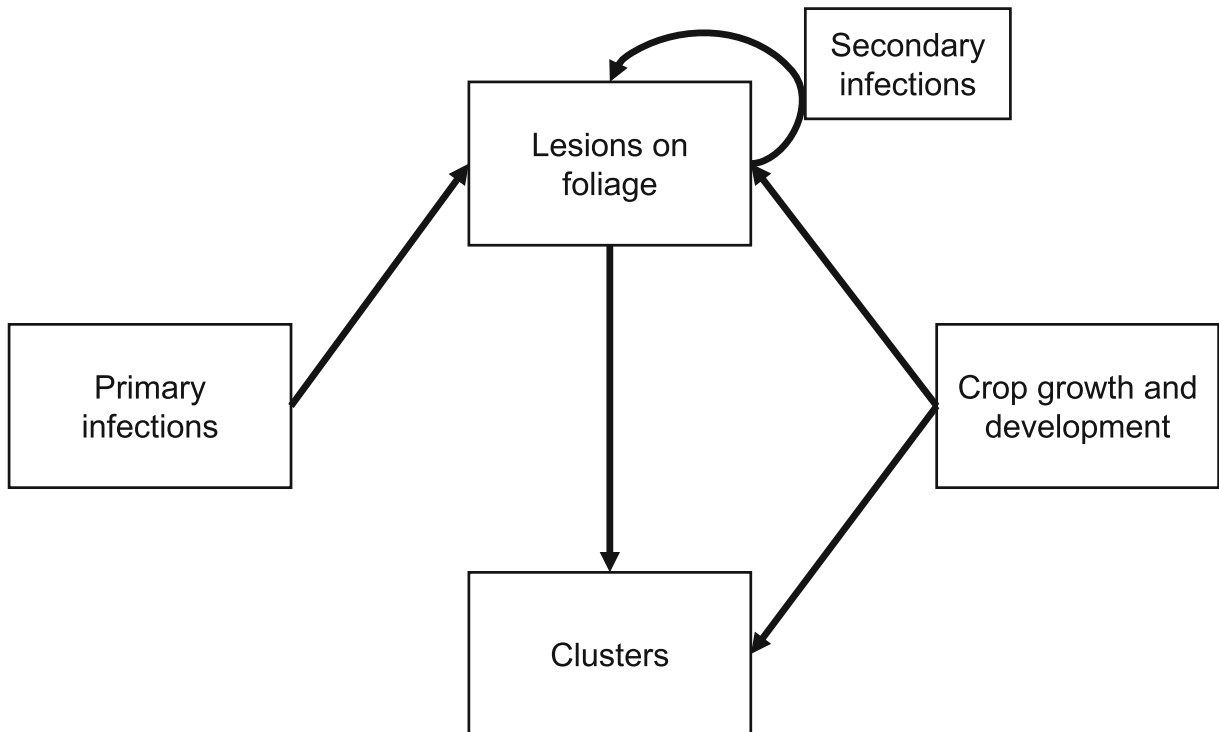


Fig. 1 Relationships among the main elements of the grape downy mildew model. Primary infections increment the number of lesions on leaves. Lesions on leaves produce secondary infections on leaves and infections on clusters. Infections on clusters are not assumed to give rise to new infections on leaves or clusters. Variation in the number of sites on leaves is dynamic during the

season, and is influenced by crop growth and senescence. Sites on leaves may vary in their susceptibility with age, which is made a function of crop development. Crop development determines (1) cluster appearance (after flowering) and (2) the period during which clusters are susceptible

Primary infections

Primary infections are assumed to only occur on leaves. The inflow of primary infections into the system is represented by the rate of primary infections (RPI). RPI is a function of three components: the epidemic onset date, OD; the duration of primary inoculum mobilization, PD; and the inflow (i.e., the rate) of primary infections occurring per time step, P. Dimensions of RPI, OD, PD and P, and of all the other coefficients, parameters, rates, and variables used in the model are shown in Table 1.

Epidemic on foliage

The model represents the epidemic process on foliage as a flow of sites through successive states. State variables store the number of sites in these states: healthy (HS), latent (L), infectious (I), and removed (R). At the beginning of the simulation, all the 100 initial sites are healthy and are stored in state variable H. In the course of the

simulation, infections on foliage, both primary and secondary, occur on available healthy sites. The rate of infection (RI) is expressed as:

$$RI = RPI + R_c \times I \times COFR \tag{3}$$

where: RPI is the rate of primary infection, R_c is the basic infection rate corrected for removals (eq. 2), and COFR is the correction factor. COFR ranges from 0 to 1 and is calculated as:

$$COFR = 1 - (D / (D + HS)) \tag{4}$$

where: D is the sum of diseased sites: $D = (L + I + R)$.

Once infected, sites become latent and thus flow from the healthy (HS), to the latent (L) and later on to the infectious (I) state. Sites remain in the latency and infectious stages for specified time durations, i.e., the latency period (LP) and infectious period (IP), respectively. Both LP and IP are set to fixed values in the course of the epidemic in the present version of the model.

Table 1 List of state variables, rates and parameters used in the model, together with their respective dimension

Symbol	Meaning of symbol	Dimension ^a
CCS	Coefficient for clusters susceptibility	[1]
CCSmax	Coefficient for clusters maximum susceptibility	[1]
COFR	Correction factor for leaves	[1]
COFRC	Correction factor for clusters	[1]
D	Total number of diseased sites on foliage	[N _{site}]
Daily T	Daily temperature	[K]
DC	Number of diseased clusters	[N _{clusters}]
DVS	Development stage	[1]
HC	Number of healthy clusters	[N _{clusters}]
HS	Number of healthy sites	[N _{site}]
I	Number of infectious sites	[N _{site}]
IP	Infectious period duration	[T]
L	Number of latent sites	[N _{site}]
LP	Latency period duration	[T]
OD	Onset date for primary infections	[T]
P	Daily inflow of primary infections	[N·T ⁻¹]
PD	Duration of mobilization of primary inoculum	[T]
R	Number of removed sites	[N _{sites}]
R _c	Number of daughter lesions per mother lesion per unit time (corrected basic infection rate)	[N _{les} ·N _{les} ⁻¹ ·T ⁻¹]
R _{cA}	Modifier for R _c related to leaf ageing	[1]
R _{cOPT}	Optimum R _c	[N _{les} ·N _{les} ⁻¹ ·T ⁻¹]
R _{cT}	Modifier of R _c for temperature	[1]
R _{cV}	Modifier of R _c for variety	[1]
R _{cW}	Modifier of R _c for moisture	[1]
RG	Rate of (foliage) growth	[N _{site} ·T ⁻¹]
RPI	Rate of primary infection	[N·T ⁻¹]
RRDS	Relative rate of disease-induced senescence	[N·N ⁻¹ ·T ⁻¹]
RRG	Relative rate of growth	[N·N ⁻¹ ·T ⁻¹]
RRS	Relative rate of senescence	[N·N ⁻¹ ·T ⁻¹]
RRSmax	Maximum relative rate of senescence	[N·N ⁻¹ ·T ⁻¹]
RSEN	Rate of senescence of healthy sites	[N _{site} ·T ⁻¹]
RSENR	Rate of senescence of removed sites	[N·T ⁻¹]
RSumT	Rate of accumulation of daily temperature	[K·T ⁻¹]
SEN	Number of healthy senesced sites	[N _{site}]
SENR	Number of removed senesced sites	[N _{site}]
Smax	Maximum number of (foliage)sites	[N]
SumT	Sum of temperature	[K]
Tbase	Base temperature for grapevine development	[K]
TC	Foliage – cluster disease transmission coefficient	[N _{cluster} ·N _{sites} ⁻¹ ·T ⁻¹]
TOTSITES	Total number of (foliage) sites present in the system	[N]

Sporulating sites on leaves (I) generate secondary infections on leaves for the duration of their infectious period (IP). The number of daughter lesions generated

per mother lesion per time step is the basic infection rate corrected for removals, R_c. R_c is expressed in the model as the product of an optimum value, R_{cOPT}, with a

series of modifiers (Loomis and Adams 1983; Savary et al. 2012, 2015), each modifier corresponding to the effects of four factors on R_c : mean temperature, moisture, leaf age and plant development stage, and varietal susceptibility. We therefore write:

$$R_c = R_{cOPT} \times R_{cT} \times R_{cW} \times R_{cA} \times R_{cV} \quad (5)$$

where R_{cT} , R_{cW} , R_{cA} , and R_{cV} are modifiers of R_{cOPT} for temperature, moisture, leaf age and plant development stage, and variety, respectively. All modifiers are bound between 0 and 1, and may therefore lead to values of R_c which are lower than R_{cOPT} .

Infections on clusters

Sporulating (i.e., infectious) sites on leaves (I) also generate infection on clusters, by means of a transmission coefficient (TC) (Savary et al. 2009). The rate of cluster infections (RCI) is calculated as:

$$RCI = TC \times I \times COFRC \times CCS \quad (6)$$

where: COFRC is the correction factor for infection on clusters, representing the proportion of healthy clusters still available for new infection; and CCS is the coefficient of cluster susceptibility. COFRC is bound between 0 and 1 and is calculated as:

$$COFRC = 1 - (DC / (DC + HC)) \quad (7)$$

where: DC and HC represent the numbers of diseased and healthy clusters, respectively.

CCS represents the development-dependent variation of cluster susceptibility, varying between 0 and 1 as a function of the development stage: CCS is 0 when DVS = 0; 1 when DVS = 1; and 0.1 when DVS is 2 (Kennelly et al. 2005).

Crop development and growth

The model considers three broad grapevine development stages (DVS): from bud break till flowering (DVS = 0); from flowering to veraison (DVS = 1); and after veraison till leaf-fall (DVS = 2). DVS values are set according to the running sum of daily temperatures (SumT) above the temperature threshold for grapevine development (Tbase). The rate of increase of SumT is RSumT, and is computed at each time step (see paragraph 2.6.) as:

$$RSumT = DailyT - Tbase$$

where: DailyT is assumed to be equal to 15 °C in the present work and Tbase is equal to 10 °C (Gutierrez et al. 1985; Winkler et al. 1974). DVS is then computed using two successive thresholds of temperature sum, as follows: DVS = 0 if SumT < 300; DVS = 1 if 300 ≤ SumT < 700; DVS is 2: if SumT ≥ 700.

The growth of the number of host sites on the foliage follows a logistic shape. The rate of foliage growth (RG) is a function of the relative rate of growth (RRG), the number of healthy sites (HS), the fraction of the current total number of sites (TOTSITES), and the maximum number of sites supported by the system (Smax), as follows:

$$RG = RRG \times HS \times (1 - (TOTSITES / Smax)) \quad (8)$$

where: TOTSITES is the sum of healthy (H), diseased (D) and senesced-removed sites (SENR), i.e., TOTSITES = H + D + SENR. When TOTSITES approaches Smax, the system approaches its carrying capacity and, thus, RG approaches 0. Note that eq. (8) assumes that only healthy sites (H) contribute to foliage growth.

Physiological senescence is represented by a rate of loss of healthy sites (RSEN) occurring between veraison and leaf-fall (i.e., when DVS = 2). RSEN represents the process whereby the number of (physiologically) senesced sites (SEN) increases proportionally with the number of healthy sites with a relative rate of senescence (RRS):

$$RSEN = RRS \times HS \quad (9)$$

The model also considers disease-induced senescence. The relative rate for disease-induced senescence, RRDS, is assumed to be greater than the relative rate for physiological senescence (RRS) (Goidanich 1959). Senescence in diseased tissues starts with the occurrence of disease and is independent from DVS. The process is considered to only affect the infected-removed, i.e., post-infectious (R), sites while the latent (L) and infectious (I) sites are not affected by disease-induced senescence, being in short transitory stages compared to the duration of a growing season. The number of removed-senesced sites (SENR) increases proportionally to the amount of removed sites (R) with a rate of senescence for the removed, RSENR, equal to:

$$RSENR = (RRS + RRDS) \times R \quad (10)$$

Initial evaluation

A numerical evaluation was conducted in order to verify whether the response of the model to variation of its main epidemiological parameters follows the expectations based on the blueprint we developed.

The parameters of the “epidemiological quintuplet” discussed by Zadoks and Schein, (1979) were considered: 1) N , the daily production of effective propagules; 2) E , the infection efficiency of propagules; 3) p , the duration of the latency period; 4) i , the duration of the infectious period; and 5) x_0 , the size of the primary inoculum.

The first and second parameters (N and E) are incorporated in the model as their product, R_cOPT (eq. 2; Zadoks 1971). Three values of R_cOPT were used for the numerical evaluation: 0.25, 0.30, and 0.35. The third and fourth parameters, p and i , correspond to LP and IP in the model; and two values were tested for each parameter: 4.8 and 7.2 for LP, and 12 and 18 for IP, which correspond to their default values, 6 and 15, respectively, increased or decreased by 20%. The fifth parameter, x_0 , is the daily flow of primary infections, P ; three values of P were tested: 0.05, 0.1 and 0.2.

A total of 48 runs were performed, resulting from the combination of the three values of R_cOPT , two of LP and IP, and three of P . To understand the effect of changes in each parameter, disease progress was calculated as the average of runs in which the parameter remains constant. For instance, disease progress curve for $R_cOPT = 0.25$ was the average of the 12 runs in which $R_cOPT = 0.25$, LP = 4.8 and 7.2, IP = 12 and 18, and $P = 0.05, 0.10$ and 0.20. The area under disease progress curve (AUDPC) was finally calculated for each model run, following Campbell and Madden (1990), and the final value of disease incidence on the clusters was computed for each run.

Results

The relational diagram of the model corresponding to its specifications, assumptions and requirements is shown in Fig. 2. The diagram was drawn following the systems representation of (Forrester 1997) as used in STELLA® (abbreviation of Systems Thinking, Experimental Learning Laboratory with Animation), a visual programming language for system dynamics modelling. The diagram combines: state variables (rectangles),

flows (solid arrows), rates (valves), parameters and coefficients (circles), and numerical relationships (dashed arrows). Acronyms of state variables, rates and parameters are listed in Table 1.

State variables

State variables consist of the sites present on leaves and of clusters. The sites on foliage are split in six dynamic, non-overlapping categories: healthy sites available for infection (HS); healthy but senesced sites not available for infection (SEN); diseased sites being latent (L), infectious (I), or removed (R), and removed senesced sites (SEN_R). Grape clusters are represented by two state variables: healthy (HC) or diseased (DC). A key element of the model is the feedback from the infectious sites (I) to the rate of infection (RI) on the foliage; this feedback accounts for the polycyclic disease increase on foliage.

Two additional variables were added to the model structure to enable (daily) computations of: SumT, sum of daily temperature and AUDPC, the area under disease progress curve on foliage, with a rate of increase computed as the (daily) sum of diseased sites: $D = L + I + R$.

Flows

Flows enable the increase or decrease of state variables. On foliage, the increase in healthy sites occurs because of host growth; its decrease occurs because of infection or senescence. The flow leaving the removals (R) represents a decrease of removed sites resulting from disease-induced senescence. The flow from healthy (HC) to diseased (DC) clusters represents the depletion of healthy clusters resulting from infection of clusters.

Rates

Rates regulate flows and are represented in the flowchart as valves (Fig. 2) RG is the rate of crop (foliage) growth (eq. 8) and regulates the increase in number of healthy sites (HS) on foliage. RI is the rate of foliage infection (eq. 3), i.e., the number of sites changing from healthy (HS) into latent (L) during a given time step. R_{trans} is the rate of transfer of sites from latent to infectious, i.e., the number of sites transferred from latent (L) to infectious (I). R_{rem} is the rate of removal from infectious, i.e., the number of sites transferred from infectious (I) to

removed (R). RSEN is the rate of leaf senescence (eq. 9), i.e., the number of sites transferred from healthy and available for infection (HS) to senescent (SEN). RSENR is the rate of senescence for the removed sites on foliage (eq. 10), i.e., the number of sites transferred from removed (R) to senescent and removed (SENR). RCI is the rate of clusters infection (eq. 6) and corresponds to the number of clusters changing from healthy (HC) into diseased (DC) during a time step.

Parameters and coefficients

Numerical values of parameters and coefficients were derived from the literature, and represent a quantitative synthesis of the available knowledge on grapevine downy mildew epidemiology.

The maximum leaf area (LA) of a grapevine plant is set to 3 m² and the number of clusters per vine is set to 20, according to values reported by Bernizzoni et al. (2009) on *Vitis vinifera* L. cv. Barbera, planted at 2.5 m inter-row and at 0.9 m within-row spacing in a single Guyot system. The dimension of a single site on leaves corresponds to the dimension of a single downy mildew lesion (LS), which is approximately 20 mm in diameter (Galet 1977); therefore, the average size of a site is 314.16 mm². The maximum number of sites on leaves (Smax) is then computed as follows:

$$S_{\max} = LA/LS = \left(3 \times 10^6 / \pi \times (10)^2\right) = 9549.3$$

Smax was rounded to 10,000 for the sake of simplicity. The relative rate of host growth, RRG, is set to 0.1 [N.N⁻¹.T⁻¹], implying that the photosynthetic activity of each healthy site contributes to the production of 0.1 new sites at each time step (Savary and Willocquet 2014). Both Smax and RRG are linked to the rate of growth (RG) as described in eq. (8). The relative rate of foliage senescence, RRS is set to 0 when DVS = 0 or DVS = 1, and to 0.01 [N.N⁻¹.T⁻¹] (represented as RRSmax in Fig. 2) when DVS = 2 (Wermelinger and Koblet 1990). The relative rate of diseased-induced senescence, RRDS, is set to 0.02 [N.N⁻¹.T⁻¹], assuming that diseased sites senesce at a rate twice that of healthy ones.

R_cOPT is the optimum value of R_c (eq. 5), i.e., the R_c under optimal, non-limiting conditions for DM; the value of R_cOPT was set to 0.3; therefore assuming that 0.3 daughter lesions are produced per mother lesion per unit time [N_{les}.N_{les}⁻¹.T⁻¹]. The value of R_c was

calculated from data in Gessler and Blaise (1992), Jermini et al. (2000), Dagostin et al. (2011), and Carisse (2016), using the approach proposed by Sun and Zeng (1994). Modifiers of R_cOPT are linked to R_c according to eq. (5). The modifiers for temperature and moisture (R_cT and R_cW) are set to 1, assuming optimal temperature and moisture conditions for the disease. The modifier for the variety, R_cV, is also set to 1, meaning that the host plant is fully susceptible to DM. The modifier for crop age (R_cA) was set as follows: R_cA = 1 if DVS = 0; R_cA = 0.56 if DVS = 1; R_cA = 0.39 if DVS = 2, meaning that the susceptibility of the foliage to DM is maximum between bud break and flowering, and then decreases when crop ages (Reuveni 1998).

The duration of latency (LP) and infectious (IP) periods is set at 6 (Goidanich 1959; Müller and Sleumer 1934) and 15 days (Caffi et al. 2013; Kennelly et al. 2007), respectively, under the assumption of optimal temperature and moisture conditions.

The daily inflow of primary infections (P) is set to 0.2 [N.T⁻¹] (Gobbin et al. 2005; Rumbou and Gessler 2004), the time of epidemic onset (OD, i.e., the day of the first seasonal infection) is fixed at DOY 120 (May 1st), i.e., OD = 30 (Rossi et al. 2008), and the duration of primary inoculum mobilization (PD, i.e., the duration over which primary infections contribute to the epidemic) is set to 60 days (Gobbin et al. 2005; Rossi et al. 2009; Rumbou and Gessler 2004).

The foliage-cluster disease transmission coefficient (TC) is set to 0.01 [N_{dc}.N_{ds}⁻¹.T⁻¹], according to Savary et al. (2009), meaning that each infectious site [N_{ds}] on foliage (I) generates 0.01 diseased cluster [N_{dc}] per time step. TC contributes to the rate of cluster infection, RCI, according to eq. (6), and thus, is modulated by the coefficient of cluster susceptibility, CCS, which makes cluster susceptibility vary from 0 (susceptibility is nil) to 1 (i.e., CCSmax, full susceptibility).

Evaluation of the model

Responses of the model to varying values of R_cOPT, LP, IP, and P are shown in Fig. 3, considering two outputs: the number of diseased sites on foliage (Fig. 3S; left panel) and the number of diseased clusters (Fig. 3C; right panel).

The dynamics of diseased sites on foliage (Fig. 3S) reflect the increase caused by infection and the growth of foliage, as well as the decrease resulting from the progressive reduction of the foliage growth rate and the

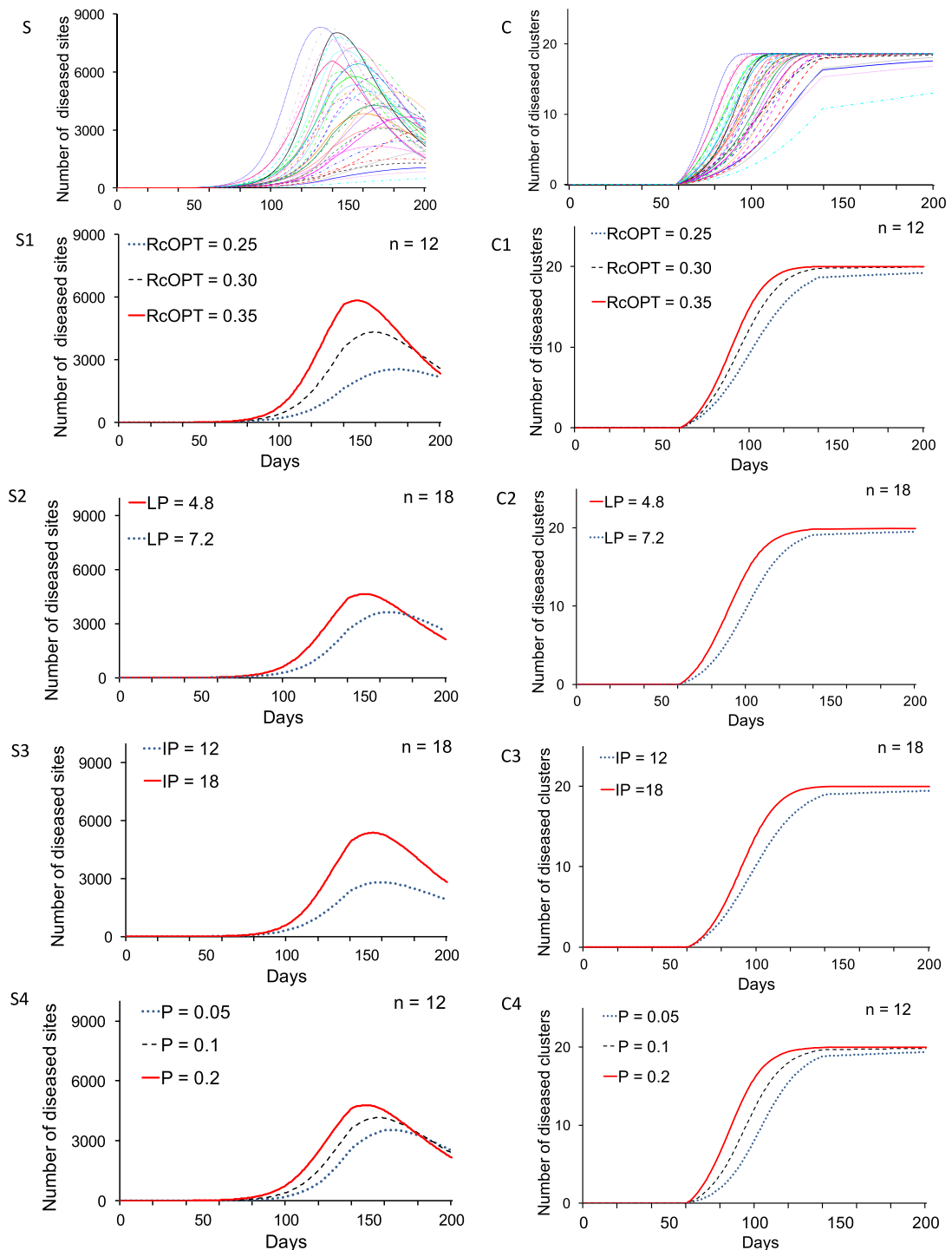


Fig. 3 Analyses of variation in the optimum daily multiplication factor (R_{cOPT}), latency period (LP), infectious period (IP) and the inflow of primary infections per day (P). Simulated numbers of diseased sites on foliage (D) are displayed in graphs on the left. Simulated number of diseased clusters (DC) are shown in graphs on the right. **S** and **C**: effects of R_{cOPT} , LP, IP and P on, respectively, the amount of disease on the foliage and the number of diseased clusters. **S1**, **S2**, **S3**, **S4**: effects of varying, respectively,

R_{cOPT} , LP, IP and P values on the number of diseased sites on foliage. Horizontal axis: time (days); vertical axis: number of diseased sites on foliage. **C1**, **C2**, **C3**, **C4**: effects of varying, respectively, R_{cOPT} , LP, IP and P values on the number of diseased clusters. Horizontal axis: time (days); vertical axis: number of diseased clusters. Values of parameters which are varied are indicated in the legend in each graph

increase of senescence. The highest number of diseased sites in the different simulation runs ranges from 100 to 8,000, i.e., never reaches the carrying capacity of the

system, 10,000 sites. The variability in the disease progress curves of Fig. 3S suggests that all four

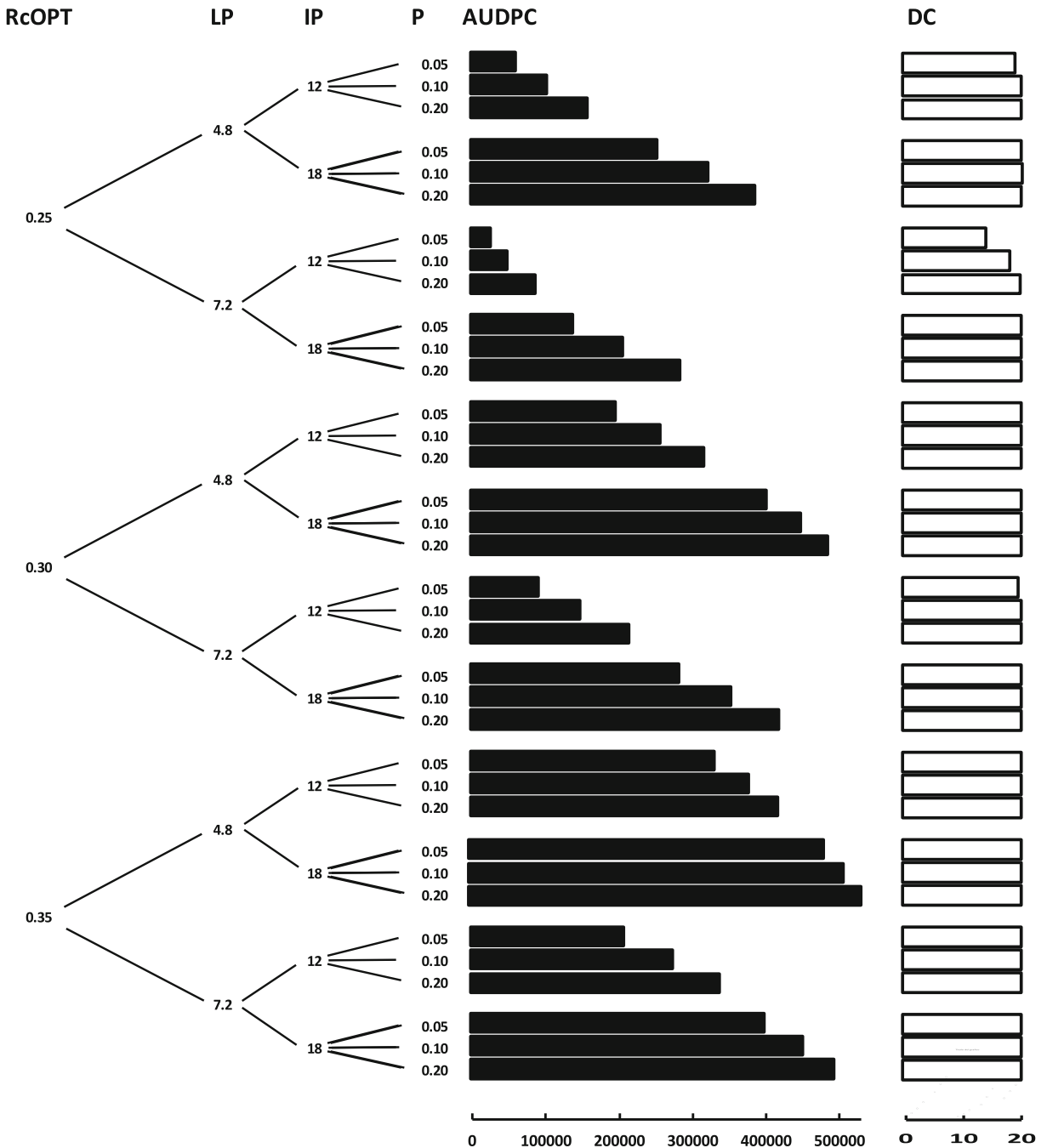


Fig. 4 Numerical evaluation: AUDPC on foliage and disease on clusters. Sensitivity analyses of variation in four parameters: a) optimum basic infection rate corrected for the removals (R_cOPT), b) latency period (LP), c) infectious period (IP) and d) the number of primary infections per day (P). The output of each run is shown

through black bars (on the left) representing the area under (foliage) disease progress curve (AUDPC) and white bars (on the right) representing the final ($t=200$) number (0–20) of diseased clusters

epidemiological parameters have effects, which are measured as changes in the AUDPC, as shown in Fig. 4.

Figure 3 S1, S2, S3, and S4 show disease progress when one of the four epidemiological parameters is changed in turn. A reduction in values of R_c OPT from 0.35 to 0.30, and to 0.25 (Fig. 3 S1), results in a strong reduction in the slope of the epidemic and, consequently, in the total disease on foliage. A 50% increase in the duration of latency (LP = 4.8 to 7.2 days; Fig. 3 S2) and decrease of infectious (LP = 12 to 18 days; Fig. 3 S3) periods result in reduced slope of the disease progress curve and number of diseased sites, which is more apparent for IP than for LP. A reduction in the daily inflow of primary infections (P; Fig. 3 S4) delays the duration of the initial phase of disease progress. The concomitant effect on the slope of the curve depends on the change in the availability of healthy sites linked to crop growth and senescence

The dynamics of the number of diseased clusters (DC) is described by S-shaped curves (Fig. 3C). In most parameter combinations, the final number of diseased clusters reaches the carrying capacity of the system, 20 clusters per plant. Some combinations of parameter values, however, result in a slight reduction in the final number of diseased clusters. Specifically, the final number of diseased clusters is smaller for the smallest values of R_c OPT, IP, and P, in combination with the largest value of LP (Fig. 4). Change in value of any of the epidemiological parameters, however, results in a visible change of the slope of the disease progress curve for clusters (Fig. 3 C1, C2, C3, and C4).

Discussion

The objective of this work was to develop a modelling structure enabling us to: 1) encompass the main phases of the grapevine DM epidemic, and 2) mobilize the available quantitative information on the epidemiology of DM on grapevine. The model involves hypotheses, assumptions and simplifications (Vanderplank 1963; Zadoks 1971). The structure of the resulting model is congruent with the initial specifications and is constructed according to our blueprint.

The model structure considers few but critical processes (specification 1). Epidemics start when a downy mildew primary infection occurs at a given onset date (OD), on a disease-free and healthy (susceptible) site (HS). After a latency period of LP

days spores are produced on the infected site and continue to be produced during an infectious period of IP days. During the infectious period, R_c effective spores per day are produced on the infectious site. Each effective spore, in turn, generates a new infection, which after LP days starts producing R_c new effective spores per day for IP days, and so on. Over the period of mobilization of primary inoculum (PD), primary infections also continue to contribute to the epidemic. These processes lead to an increase in the total number of downy mildew lesions on the foliage, which is governed by the system size, host foliage (crop) growth, physiological and disease-induced senescence, susceptibility of plant organs, age of organs, and environmental factors. The infection of clusters mirrors the foliage epidemic and is introduced in the model as a simple set of relationships. These processes make the overall structure of the model relatively simple, transparent and generic, so that it can be shared and used for several purposes. The structure of the model can be easily modified and adapted to other pathosystems with similar characteristics, e.g., some scab diseases, some powdery mildews and others originating polycyclic, dual epidemics (Savary et al. 2009) developing on two populations of organs.

Despite its simplicity, the model accounts for the complexity of the pathosystem under consideration. This complexity first originates from the life cycle of *P. viticola* itself, with its dimorphism in the primary and secondary inoculum, resulting in three phases of the epidemic driven by primary spores (macrosporangia), by both primary and secondary (sporangia) spores, and by secondary spores only, respectively (Rossi et al. 2009; Rossi et al. 2013). A second element of complexity is the dual character of the epidemic, since *P. viticola* infects both leaves and clusters. Third, DM epidemics last a very long period of time every season, potentially running from early spring, when the first seasonal leaf is unfolded and has functional stomata (Emmett et al. 1992), to fall, when the foliage is fully senescent and no living tissue is available for supporting the obligate growth of the pathogen (Grünzel 1961). A fourth element is the ontogenic resistance of the host tissue, which encompasses both leaves and bunches (Ficke et al. 2002; Gadoury 2015; Kennelly et al. 2005). A last element of complexity is associated with the genetic resistance of the grapevine, which may affect different epidemiological components and acts on the disease

throughout a season and over the entire epidemic (Jeger et al. 1983; Parlevliet 1979; Zadoks 1977).

The previous published models on grape downy mildew did not incorporate all this complexity, many of them focusing on some particular phases of the epidemic only. For instance, the models developed by Rossi et al. (2008), Hill (2000), and Park et al. (1997) consider primary infections. Other models only account for secondary infections (Blaise et al. 1999; Ellis et al. 1994; Kassemeyer 1994; Lalancette et al. 1988; Magarey et al. 1991; Orlandini et al. 1993). The model of Rossi et al. (2009) incorporates quantitative aspects of both primary and secondary infections, but does not consider the dual nature of the epidemics.

The model structure developed in this work incorporates the main host crop processes (specification 2), in particular: i) crop growth and senescence, which influence the dynamics of healthy sites available for new infections, and ii) physiological development (age) of grapevine organs in a growing seasons, which influences the susceptibility of both the foliage and clusters. The modelled system consists of a single grapevine plant, that is, a suitable system size to account for all the plant organs involved in the DM epidemic, i.e. foliage and clusters, and for the main disease processes, i.e. primary and secondary infections (specification 3).

In this paper, crop variables (leaf area, number of clusters per plant), crop physiology and development (DVS) are defined with reference to northern Italy (cultivar, training system, inter- and within-row spacing). However, the model structure is generic enough to enable parameterisation in any conditions under which grapevine is grown in the world. The approach followed in the present work involves simplifications, which correspond to a “mean field” hypothesis (Levin et al. 1997). A typical version of the mean field hypothesis is made over space: our model considers a single grapevine plant surrounded by similar systems (plants) in a steady state, that is, the plant structure and the microclimatic conditions are the same in the modelled system and in the similar surrounding systems, and there is a dynamic equilibrium in flows of spores entering and exiting the system. One implication of this hypothesis is that the probability of infection of any host site is everywhere the same within the system. The mean field hypothesis over space is a strong hypothesis, but yet is shared by many epidemiological models, which have proven to be useful research tools (Zadoks and Schein 1979).

The model considers clusters under only two categories, healthy or diseased, and this refers to disease incidence (Madden et al. 2007). At a different level of hierarchy (Willoquet and Savary 2004), clusters can be considered as composed by a number of berries, and berries can be considered healthy or diseased; this may improve the resolution of the model in explaining the dynamics of epidemics on clusters. However, considering single berries is only possible for a short period of the epidemic (Chellemi and Marois 1992; Gadoury et al. 2003; Galet 1977; Gobbin et al. 2005; Kennelly et al. 2005), i.e., from the fruit set (when berries shape) stage until the pea-sized berries stage (when stomata on the berry surface lose function and direct penetration of *P. viticola* is no longer possible; Gessler et al. 2011; Kennelly et al. 2005). Before fruit set, young clusters rapidly develop necrosis once infected, display epinasty and the entire inflorescence may die (Kennelly et al. 2007). Developing berries turn light brown to purple when infected, and shrivels, resulting in quality losses so that a lower price is paid to the grower if the clusters show even few DM symptoms. Considering these aspects, a model structure accounting for cluster incidence provides a simple but reasonable way for the purpose of the model.

The model makes additional simplification concerning the cluster infection. In reality, infection of grapevine clusters may take place through three different processes: i) primary inoculum splashing from soil in the early epidemic stage; ii) secondary inoculum produced on leaves by asexual reproduction and dispersed onto clusters in the course of the epidemic; and iii) infection between clusters, that is, secondary infection of clusters produced by lesions present on clusters. The current model structure only accounts for the second process, and this may lead to an underestimation of the disease on clusters. There are two main reasons for this simplification. First, there is no information in the literature about the contribution of primary inoculum to overall cluster infection (Gobbin et al. 2001). A second reason is that diseased berries produce sporangia for a very short period (Kennelly et al. 2005) and the conversion of stomata to lenticels after infection may prevent sporulation (Kennelly et al. 2007); therefore, the contribution of the third process may be negligible compared to the second. Furthermore, the transmission rate of the disease from leaves to clusters used into the model Savary et al. (2009) is derived from disease transmission equations from leaves to clusters based on actual field

assessments of disease on leaves and clusters. These equations, and therefore our transmission parameter, implicitly include all three processes.

The model is conceived to respond to the main environmental variables that influence the functioning of the system (specification 4). Specifically, modifiers R_cT and R_cW respectively account for the effect of temperature and moisture on R_c . Additional modifiers can easily be introduced into the model structure, accounting for the effect of weather conditions on other epidemiological parameters such as, for instance, the effect of temperature and moisture on the duration of mobilization of primary inoculum (PD; Rossi et al. 2008), of rain on the daily inflow of primary infections (P; Rossi and Caffi 2012), and of temperature on latency or infectious periods (LP or IP; Goidanich 1959; Hill 1989; Rossi et al. 2002). In this work, setting these parameters at fixed values is a simplification referring to the mean field hypothesis over time (Levin et al. 1997).

The system is modelled within a time frame of 200 days, which is sufficient to address all downy mildew processes during a grapevine-growing season (specification 5). The model runs with a time step of one day, allowing simulating disease and crop processes in a continuous way (specification 6). The choice of a daily time step leads to collapsing those epidemiological processes that take place in quite smaller time constants (Savary et al. 2018; Zadoks 1971). For instance, the stages leading to primary infections include: oospore germination, formation of primary zoosporangia (macrosporangia), release of zoospores from macrosporangia, dispersal of zoospores by rain splashes from the soil to the canopy, deposition of zoospores onto leaves, swimming of the zoospores to stomata, germination and penetration through stomata (Rossi et al. 2009). The choice of a one-day time step then implies the assumption that all these processes occurring in a time period shorter than one day are collapsed. This assumption is in line with many epidemiological studies (Savary et al. 2018), and in agreement with the overall objectives of the model.

The numerical evaluation shows that the model performs according to expectations. The overall behaviour of the model, the flexibility of responses to four interacting parameters shown in Fig. 3 conform to the hypotheses associated with its development. As expected, increasing the basic infection rate under optimal conditions (R_{cOPT}), increasing the duration of infectious period (IP), and decreasing the duration of the

latency period (LP) all result in a faster increase of the epidemic on both foliage and clusters, as described by eq. (1). Decreasing the number of primary infections on foliage delays epidemics on foliage and on clusters. These results then conform to theory (Vanderplank 1963; Zadoks 1971; Zadoks and Schein 1979). We note, however, the strong effect of (increasing) IP on the shape of disease progress curve (Fig. 3). Compared to other modelling structures (Savary et al. 2018; Zadoks 1971; Zadoks and Schein 1979) this response is particularly strong and reflects the interplay of IP with other parameters of the model related to crop growth and senescence.

In conclusion, this work reports a generic/conceptual simulation model that can be used for understanding: i) the effect of strategic disease management as, for instance, the use of grape varieties with different levels of partial resistance to DM or the transition of vineyard management from conventional to organic; ii) the behaviour of the pathosystem under different environmental conditions or under climate change; iii) the effect of tactical management of vineyards such as canopy management and fungicide applications strategy. The model can also be useful for the identification of knowledge gaps.

Acknowledgments This study was supported by the Doctoral School on the Agro-Food System (Agrisystem) of the Università Cattolica del Sacro Cuore (Italy).

Compliance with ethical standards The Authors declare that the present manuscript complies with the Ethical Rules of good scientific practice applicable for the European Journal of Plant Pathology.

Conflict of interest The authors declare that they have no conflict of interest. All authors are informed and agree on the publication of the manuscript.

Research involving human participants and/or animals Not applicable, the research does not involve humans or animals.

Informed consent Not applicable, the research does not involve human participants.

References

- Allorant, D., & Savary, S. (2005). Epidemiological characteristics of angular leaf spot of bean: A systems analysis. *European Journal of Plant Pathology*, 113(4), 329–341. <https://doi.org/10.1007/s10658-005-4038-y>.

- Allorent, D., Willocquet, L., Sartorato, A., & Savary, S. (2005). Quantifying and modelling the mobilisation of inoculum from diseased leaves and infected defoliated tissues in epidemics of angular leaf spot of bean. *European Journal of Plant Pathology*, 113(4), 377–394. <https://doi.org/10.1007/s10658-005-4269-y>.
- Avelino, J., Allinne, C., Cerda, R., Willocquet, L., & Savary, S. (2018). Multiple-disease system in coffee: From crop loss assessment to sustainable management. *Annual Review of Phytopathology*, 56(1), 611–635. <https://doi.org/10.1146/annurev-phyto-080417-050117>.
- Bernizzoni, F., Gatti, M., Civardi, S., & Poni, S. (2009). Long-term performance of Barbera grown under different training systems and within-row vine spacings. *American Journal of Enology and Viticulture*, 60(3), 339–348.
- Blaise, P., Dietrich, R., & Gessler, C. (1999). VINEMILD: An application-oriented model of *Plasmopara viticola* epidemics on *Vitis vinifera*. In Wagenmakers, Van der Werf, & Blaise (Eds.), *Acta Horticulture ISHS IOBC/WPRS Bulletin I* (pp. 187–192).
- Bove, F. (2018). A modelling framework for grapevine downy mildew epidemics incorporating foliage-cluster relationships and host plant resistance. Università Cattolica del Sacro Cuore, Piacenza, Italy. Retrieved from <http://hdl.handle.net/10280/57899>
- Bove, F., Savary S., Willocquet L., Rossi V. (Submitted). Simulation of potential epidemics of downy mildew of grapevine in different scenarios of disease conduciveness.
- Caffi, T., Legler, S. E., Rossi, V., & Poni, S. (2010). Photosynthetic activity in grape leaf tissue with latent, visible and “virtual” downy mildew lesions. In Proceedings of the “6th international workshop on grapevine downy and powdery mildew” (pp. 60–62). Bordeaux: INRA.
- Caffi, T., Gilardi, G., Monchiero, M., & Rossi, V. (2013). Production and release of asexual sporangia in *Plasmopara viticola*. *Phytopathology*, 103(1), 64–73. <https://doi.org/10.1094/PHYTO-04-12-0082-R>.
- Campbell, C. L., & Madden, L. V. (1990). *Introduction to plant disease epidemiology*. New York: John Wiley & Sons.
- Carisse, O. (2016). Development of grape downy mildew (*Plasmopara viticola*) under northern viticulture conditions: Influence of fall disease incidence. *European Journal of Plant Pathology*, 144(4), 773–783. <https://doi.org/10.1007/s10658-015-0748-y>.
- Chellemi, D. O., & Marois, J. J. (1992). Influence of leaf removal, fungicide applications, and fruit maturity on incidence and severity of grape powdery mildew. *American Journal of Enology and Viticulture*, 43(1), 53 LP – 57. <http://www.ajevonline.org/content/43/1/53.abstract>
- Dagostin, S., Schärer, H. J., Pertot, I., & Tamm, L. (2011). Are there alternatives to copper for controlling grapevine downy mildew in organic viticulture? *Crop Protection*, 30(7), 776–788. <https://doi.org/10.1016/j.cropro.2011.02.031>.
- Develey-Rivière, M. P., & Galiana, E. (2007). Resistance to pathogens and host developmental stage: A multifaceted relationship within the plant kingdom. *New Phytologist*, 175(3), 405–416. <https://doi.org/10.1111/j.1469-8137.2007.02130.x>.
- Ellis, M. A., Madden, L. V., & Lalancette, N. (1994). A disease forecasting program for grape downy mildew in Ohio. *Special report (New York State Agricultural Experiment Station)*, 68, 92–95.
- Emmett, R. W., Wicks, T. J., & Magarey, P. A. (1992). Downy mildew of grapes. *Plant diseases of international importance. Volume III. Diseases of fruit crops*. Englewood Cliffs: Prentice Hall.
- Farrar, J. F. (1992). Beyond photosynthesis: The translocation and respiration of diseased leaves. In *Pests and Pathogens. Plant Responses to Foliar Attack*. (Ayres PG., pp. 102–127). Oxford: Bios Scientific Publishers.
- Ficke, A., Gadoury, D. M., & Seem, R. C. (2002). Ontogenic resistance and plant disease management: A case study of grape powdery mildew. *Phytopathology*, 92(6), 671–675. <https://doi.org/10.1094/PHYTO.2002.92.6.671>.
- Forrester, J. W. (1997). Industrial dynamics. *Journal of the Operational Research Society*, 48(10), 1037–1041. <https://doi.org/10.1057/palgrave.jors.2600946>.
- Gadoury, D. M. (2015). Climate, asynchronous phenology, ontogenic resistance, and the risk of disease in deciduous fruit crops. In *IOBC/WPRS Bulletin* (Vol. 110, pp. 15–24).
- Gadoury, D. M., Seem, R. C., Ficke, A., & Wilcox, W. F. (2003). Ontogenic resistance to powdery mildew in grape berries. *Phytopathology*, 93(5), 547–555. <https://doi.org/10.1094/PHYTO.2003.93.5.547>.
- Galet, P. (1977). *Les Maladies et les Parasites de la Vigne. Vol 1*. Montpellier: Imprimerie du Paysan du Midi.
- Gessler, C., & Blaise, P. (1992). An extended progeny/parent ratio model II. Application to experimental data. *Journal of Phytopathology*, 134(1), 53–62. <https://doi.org/10.1111/j.1439-0434.1992.tb01211.x>.
- Gessler, C., Pertot, I., & Perazzolli, M. (2011). *Plasmopara viticola*: a review of knowledge on downy mildew of grapevine and effective disease management. *Phytopathologia Mediterranea*, 50(1), 3–44. <http://hdl.handle.net/10449/20124>.
- Giuntoli, A., & Orlandini, S. (2000). Effects of downy mildew on photosynthesis of grapevine leaves. *Acta Horticulture*, 526, 461–466.
- Gobbin, D., Jermini, M., & Gessler, C. (2003). The genetic underpinning of the minimal fungicide strategy. In *Integrated Protection and Production in Viticulture IOBC wprs Bulletin* (Vol. 26, pp. 101–104). http://www.iobc-wprs.org/pub/bulletins/iobc-wprs_bulletin_2003_26_08.pdf#page=295
- Gobbin, D., Jermini, M., Loskill, B., Pertot, I., Raynal, M., & Gessler, C. (2005). Importance of secondary inoculum of *Plasmopara viticola* to epidemics of grapevine downy mildew. *Plant Pathology*, 54(4), 522–534. <https://doi.org/10.1111/j.1365-3059.2005.01208.x>.
- Goidanich, G. (1959). *Manuale di patologia vegetale - v. 1–4*. Bologna (Italy): Edizioni Agricole.
- Grünzel, H. (1961). Untersuchungen über die Oosporenbildung beim Falschen Mehltau der Weinrebe (*Peronospora viticola* de Bary). *Zeitschrift für Pflanzenkrankheiten (Pflanzenpathologie) und Pflanzenschutz*, 68(2), 65–80 <http://www.jstor.org/stable/43231828>.
- Gutierrez, A. P., Williams, D. W., & Kido, H. (1985). A model of grape growth and development: The mathematical structure and biological considerations. *Crop Science*, 25(5), 721–728. <https://doi.org/10.2135/cropsci1985.0011183x002500050001x>.
- Hill, G. K. (1989). Effect of temperature on sporulation efficiency of oilspots caused by *Plasmopara viticola* (Berk. & Curt. Ex

- De Bary) Berl. & De Toni in the vineyard. *Viticultural and Enological Sciences*, 44, 86–90.
- Hill, G. K. (1990). Studies on *Plasmopara viticola* epidemics in the vineyard. In Atti del Convegno su Modelli Euristici ed Operativi in Agricoltura (pp. 266–273). Caserta (Italy): Societa Italiana di Fitoiatria.
- Hill, G. K. (2000). Simulation of *P. viticola* oospore-maturation with the model SIMPO. *Bulletin OILB/SROP*, 23(4), 7–8.
- Jeger, M. J. (1984). Relating disease progress to cumulative numbers of trapped spores: Apple powdery mildew and scab epidemics in sprayed and unsprayed orchard plots. *Plant Pathology*, 33(4), 517–523. <https://doi.org/10.1111/j.1365-3059.1984.tb02876.x>.
- Jeger, M. J., Gareth Jones, D., & Griffiths, E. (1983). Components of partial resistance of wheat seedlings to *Septoria nodorum*. *Euphytica*, 32(2), 575–584. <https://doi.org/10.1007/BF00021470>.
- Jermini, M., Dietrich, R., Aerni, J., & Blaise, P. (2000). Early control of grapevine downy mildew allows a reduction of fungicide application. In *Integrated Control in Viticulture IOBC/WPRS Bulletin* 23, 3–6.
- Kassemeyer, H. H. (1994). Experience with electronic warning of downy mildew of grapevine. In D. M. Gadoury & R. C. Seem (Eds.), *Proc. Int. Workshop Grapevine Downy Mildew Modeling, 1st.* (pp. 80–81). N.Y. Agric. Exp. Stn. Spec. Rep. 68.
- Kennelly, M. M., Gadoury, D. M., Wilcox, W. F., Magarey, P. A., & Seem, R. C. (2005). Seasonal development of ontogenic resistance to downy mildew in grape berries and rachises. *Phytopathology*, 95(12), 1445–1452. <https://doi.org/10.1094/PHYTO-95-1445>.
- Kennelly, M. M., Gadoury, D. M., Wilcox, W. F., Magarey, P. A., & Seem, R. C. (2007). Primary infection, lesion productivity, and survival of sporangia in the grapevine downy mildew pathogen *Plasmopara viticola*. *Phytopathology*, 97(4), 512–522. <https://doi.org/10.1094/PHYTO-97-4-0512>.
- Kranz, J. (1979). Simulation of epidemics caused by *Venturia inaequalis* (Cooke) Aderh. *EPPO Bulletin*, 9(3), 235–242. https://doi.org/10.1007/978-3-642-96220-2_7.
- Kranz, J., & Hau, B. (1980). Systems analysis in epidemiology. *Annual Review of Phytopathology*, 18(1), 67–83. <https://doi.org/10.4324/9781315123806>.
- Lalancette, N., Madden, L. V., & Ellis, M. A. (1988). A quantitative model for describing the sporulation of *Plasmopara viticola* on grape leaves. *Phytopathology*, 78(10), 1316–1321. <https://doi.org/10.1094/phyto-78-1316>.
- Leroy, P., Smits, N., Cartolaro, P., Delière, L., Goutouly, J. P., Raynal, M., & Alonso Ugaglia, A. (2013). A bioeconomic model of downy mildew damage on grapevine for evaluation of control strategies. *Crop Protection*, 53, 58–71. <https://doi.org/10.1016/j.cropro.2013.05.024>.
- Levin, S. A., Grenfell, B., Hastings, A., & Perelson, A. S. (1997). Mathematical and computational challenges in population biology and ecosystems science. *Science*, 275(5298), 334 LP–343. <https://doi.org/10.1126/science.275.5298.334>.
- Loomis, R. S., & Adams, S. S. (1983). Integrative analyses of host-pathogen relations. *Annual Review of Phytopathology*, 21(1), 341–362. <https://doi.org/10.1146/annurev.py.21.090183.002013>.
- Lorenz, D. H., Eichhorn, K. W., Bleiholder, H., Klose, R., Meier, U., & Weber, E. (1995). Growth stages of the grapevine: Phenological growth stages of the grapevine (*Vitis vinifera* L. ssp. *vinifera*)—Codes and descriptions according to the extended BBCH scale. *Australian Journal of Grape and Wine Research*, 1(2), 100–103. <https://doi.org/10.1111/j.1755-0238.1995.tb00085.x>.
- Madden, L. V., Hughes, G., & van den Bosch, F. (2007). *The Study of Plant Disease Epidemics*. St Paul, MN: American Phytopathological society (APS press). <https://doi.org/10.1094/9780890545058.fm>.
- Magarey, P. A., Wachtel, M. F., Weir, P. C., & Seem, R. C. (1991). A computer-based simulator for rationale management of grapevine downy mildew (*Plasmopara viticola*). *Australian Plant Protection Quarterly*, 6(1), 29–33.
- Müller, K., & Sleumer, H. (1934). Biologische Untersuchungen über die Peronosporakrankheit des Weinstockes mit besonderer Berücksichtigung ihrer Bekämpfung nach der Inkubationskalendermethode. *Landwirtschaftliche Jahrbucher*, 79(4), 509–576.
- Orlandini, S., Gozzini, B., Rosa, M., Egger, E., Storch, P., Maracchi, G., & Miglietta, F. (1993). PLASMO: A simulation model for control of *Plasmopara viticola* on grapevine. *EPPO Bulletin*, 23(4), 619–626.
- Park, E. W., Seem, R. C., Gadoury, D. M., & Pearson, R. C. (1997). DMCAT: A prediction model for grape downy mildew development. *Viticultural and Enological Science*, 52(3), 182–189.
- Parlevliet, J. E. (1979). Components of resistance that reduce the rate of epidemic development. *Annual Review of Phytopathology*, 17(1), 203–222. <https://doi.org/10.1146/annurev.py.17.090179.001223>.
- Poni, S., Palliotti, A., & Bernizzoni, F. (2006). Calibration and evaluation of a STELLA software-based daily CO₂ balance model in *Vitis vinifera* L. *Journal of the American Society for Horticultural Science*, 131(2), 273–283.
- Rabbinge, R., & de Wit, C. T. (1989). Theory of modelling and systems. In *Simulation and Systems Management in Crop Protection* (pp. 3–15). Wageningen: Centre for Agricultural Publishing and Documentation (Pudoc). [https://doi.org/10.1016/0308-521x\(93\)90084-f](https://doi.org/10.1016/0308-521x(93)90084-f).
- Reuveni, M. (1998). Relationships between leaf age, peroxidase and β -1, 3-Glucanase activity, and resistance to downy mildew in grapevines. *Journal of Phytopathology*, 146(10), 525–530.
- Rossi, V., & Caffi, T. (2012). The role of rain in dispersal of the primary inoculum of *Plasmopara viticola*. *Phytopathology*, 102(2), 158–165. <https://doi.org/10.1094/PHYTO-08-11-0223>.
- Rossi, V., Bugiani, R., Girometta, B., & Giosuè, S. (2002). Funghi, batteri e virus: Influenza delle condizioni meteorologiche sulle infezioni primarie di *Plasmopara viticola* in Emilia Romagna. In A. Brunelli & A. Canova (Eds.), *Atti delle Giornate Fitopatologiche* (Vol. 2, pp. 1000–1008). Bologna: CLUEB.
- Rossi, V., Caffi, T., Giosue, S., Girometta, B., Bugiani, R., Spanna, F., et al. (2005). Elaboration and validation of a dynamic model for primary infections of *Plasmopara viticola*. *Rivista Italiana di Agrometeorologia*, 3, 7–13 <http://hdl.handle.net/10807/45996>.
- Rossi, V., Caffi, T., Giosuè, S., & Bugiani, R. (2008). A mechanistic model simulating primary infections of downy mildew

- in grapevine. *Ecological Modelling*, 212(3–4), 480–491. <https://doi.org/10.1016/j.ecolmodel.2007.10.046>.
- Rossi, V., Giosuè, S., & Caffi, T. (2009). Modelling the dynamics of infections caused by sexual and asexual spores during *Plasmopara Viticola* epidemics. *Journal of Plant Pathology*, 91(3), 615–627.
- Rossi, V., Caffi, T., & Gobbin, D. (2013). Contribution of molecular studies to botanical epidemiology and disease modelling: Grapevine downy mildew as a case-study. *European Journal of Plant Pathology*, 135(4), 641–654. <https://doi.org/10.1007/s10658-012-0114-2>.
- Royle, D. J. (1973). Quantitative relationships between infection by the hop downy mildew pathogen, *Pseudoperonospora humuli*, and weather and inoculum factors. *Annals of Applied Biology*, 73(1), 19–30. <https://doi.org/10.1111/j.1744-7348.1973.tb01305.x>.
- Rumbou, A., & Gessler, C. (2004). Genetic dissection of *Plasmopara viticola* population from a Greek vineyard in two consecutive years. *European Journal of Plant Pathology*, 110(4), 379–392. <https://doi.org/10.1023/B:EJPP.0000021061.38154.22>.
- Savary, S., & Willocquet, L. (2014). Simulation modeling in botanical epidemiology and crop loss analysis. *The Plant Health Instructor*. APSnet Education Center. <https://doi.org/10.1094/phi-a-2014-0314-01>.
- Savary, S., De Jong, P. D., Rabbinge, R., & Zadoks, J. C. (1990). Dynamic simulation of groundnut rust: A preliminary model. *Agricultural Systems*, 32(2), 113–141. [https://doi.org/10.1016/0308-521X\(90\)90034-N](https://doi.org/10.1016/0308-521X(90)90034-N).
- Savary, S., Delbac, L., Rochas, A., Taisant, G., & Willocquet, L. (2009). Analysis of nonlinear relationships in dual epidemics, and its application to the management of grapevine downy and powdery mildews. *Phytopathology*, 99(8), 930–942. <https://doi.org/10.1094/PHYTO-99-8-0930>.
- Savary, S., Nelson, A., Willocquet, L., Pangga, I., & Aunario, J. (2012). Modeling and mapping potential epidemics of rice diseases globally. *Crop Protection*, 34, 6–17. <https://doi.org/10.1016/j.cropro.2011.11.009>.
- Savary, S., Stetkiewicz, S., Brun, F., & Willocquet, L. (2015). Modelling and mapping potential epidemics of wheat diseases—Examples on leaf rust and Septoria tritici blotch using EPIWHEAT. *European Journal of Plant Pathology*, 142(4), 771–790. <https://doi.org/10.1007/s10658-015-0650-7>.
- Savary, S., Nelson, A. D., Djurle, A., Esker, P. D., Sparks, A., Amorim, L., Bergamin Filho, A., Caffi, T., Castilla, N., Garrett, K., McRoberts, N., Rossi, V., Yuen, J., & Willocquet, L. (2018). Concepts, approaches, and avenues for modelling crop health and crop losses. *European Journal of Agronomy*, 100(September 2016), 4–18. <https://doi.org/10.1016/j.eja.2018.04.003>.
- Shoemaker, C. A. (1981). Applications of dynamic programming and other optimization methods in Pest management. *IEEE Transactions on Automatic Control*, 26(5), 1125–1132. <https://doi.org/10.1109/TAC.1981.1102782>.
- Sun, P., & Zeng, S. (1994). On the measurement of the corrected basic infection rate. *Zeitschrift für Pflanzenkrankheiten und Pflanzenschutz*, 101(3), 297–302.
- Vanderplank, J. E. (1963). Plant diseases: Epidemics and control. *Academic Press Inc. (New York)*.
- Wermelinger, B., & Koblet, W. (1990). Seasonal growth and nitrogen distribution in grapevine leaves, shoots and grapes. *Vitis*, 29(1), 15–26.
- Willocquet, L., & Savary, S. (2004). An epidemiological simulation model with three scales of spatial hierarchy. *Phytopathology*, 94(8), 883–891. <https://doi.org/10.1094/PHYTO.2004.94.8.883>.
- Winkler, A. J., Cook, J. A., Kliewer, W. M., & Lider, L. A. (1974). The physiology of the vine. In *General viticulture* (pp. 90–109). Berkeley, Calif. (USA): University of California Press.
- Zadoks, J. C. (1971). Systems analysis and the dynamics of epidemics. *Phytopathology*, 61, 600–610.
- Zadoks, J. C. (1977). Simulation models of epidemics and their possible use in the study of disease resistance. In *Proceedings of a symposium on induced mutations against plant diseases* (pp. 109–118). Vienna, Austria: International Atomic Energy Agency (IAEA). http://inis.iaea.org/search/search.aspx?orig_q=RN:09373754
- Zadoks, J. C., & Rabbinge, R. (1985). Modelling to a purpose. CA Gilligan (Eds) *Advances in Plant Pathology*, mathematical Modelling of crop diseases Vol. 3 academic press London 231–244Zadoks, J. C., & Schein, R. D. (1979). *Epidemiology and plant disease management*. New York, N.Y. (USA) Oxford Univ. press.